Optical coherence tomography measurement of retinal nerve fibre layer thickness and comparison with visual field analysis in patients with primary open angle glaucoma

Dissertation submitted for
MS (Branch III) Ophthalmology

THE TAMIL NADU DR. M.G.R MEDICAL UNIVERSITY
CHENNAI

March 2006

CERTIFICATE

Certified that this dissertation entitled "**Optical coherence tomography measurement of retinal nerve fibre layer thickness and comparison with visual field analysis in patients with primary open angle glaucoma**" submitted for MS (Branch III) Ophthalmology, The Tamil Nadu Dr.M.G.R.Medical University, March 2006 is the bonafide work done by **Dr. P. M. ARAVIND**, under our supervision and guidance in the Glaucoma Services of Aravind Eye Hospital and Post Graduate Institute of Ophthalmology, Madurai during his residency period from April 2003 to March 2006.

DR. S. R. KRISHNA DAS
Chief, Glaucoma Services
Aravind Eye Hospital
    Madurai.

DR. M. SRINIVASAN
Director
Aravind Eye Hospital
    Madurai.

ACKNOWLEDGEMENT

CONTENTS

INTRODUCTION

Glaucoma is among the leading causes of irreversible blindness in the developing world and a major health problem in the developed world. [1, 2] World Health Organisation statistics indicate that glaucoma accounts for blindness in 5.1 million persons, or 13.5% of global blindness. Primary open angle glaucoma is explicitly characterized as a "multifactorial optic neuropathy with a characteristic acquired loss of optic nerve fibres", developing in the presence of open anterior chamber angles and manifesting characteristic visual field abnormalities in the absence of other known causes of the disease.[3]

Glaucoma is characterized by a gradual loss of retinal ganglion cells and thinning of the Retinal Nerve Fibre Layer (RNFL). Since glaucomatous damage is irreversible, prevention of this injury before it occurs is the essential strategy available to those treating this disease. The early diagnosis of glaucoma and the early detection of glaucomatous progression are twin central challenges facing ophthalmologists. [4]

Significant axonal loss may precede the development of visual field defects and identifiable cupping.[5] Subjective assessments of optic nerve head cupping are not sufficiently sensitive to detect small changes, especially notches and other local abnormalities, and in many cases are unable to discriminate between glaucomatous and normal optic nerve heads.[6] Drawings

of the optic nerve head and stereoscopic optic nerve head photography depend on the subjective interpretation of the examiner and are thereby subject to variability in interpretation. Current diagnostic techniques such as retinal and optic nerve head analysis instruments and stereofundus photography lack sensitivity and reproducibility.[6-10]

Optic nerve head analyzers, developed to quantitate cupping, can measure optic nerve head rim area and provide other indices of optic nerve head structure, but can not reliably differentiate between normal and glaucomatous, and are limited in their ability to detect change over time.[7-14] Improved axial resolution with reduced variability in assessing optic nerve topography is achieved with the confocal scanning laser ophthalmoscope, which produces optical sections of the retina and optic nerve head in a coronal plane. Cross-sectional imaging of the fundus with scanning laser ophthalmoscopy is limited by ocular aberrations and the pupil aperture to approximately 300 μm of axial resolution.[15]

Optical Coherence Tomography (OCT) is a non-invasive, noncontact method that allows cross-sectional, in vivo imaging of the intraretinal layers.[16] Anatomic layers within the retina can be imaged and quantitative assessment of RNFL thickness can be performed based on the different reflectivity properties of different layers.[16-18] OCT data is reported to correlate well with real

measurements of RNFL thickness. Studies also have reported a decrease in OCT RNFL thickness in glaucomatous eyes compared with healthy eyes.[19-23]

Structure-based methodologies need to ultimately compare with a gold standard, which is currently, automated perimetry. However, glaucoma patients could suffer a loss (approx. 40%) of retinal ganglion cell axons before an automated perimetry visual field defect is evident[24]. The purpose of this study is to investigate the agreement in glaucomatous damage detection between structural changes by OCT and functional alteration by automated perimetry.

REVIEW OF LITERATURE

A Medline literature search was performed using the key words "optical coherence tomography", "glaucoma" and "visual fields". The most relevant studies with respect to this dissertation were selected.

Quantification of Nerve Fibre Layer Thickness in Normal and Glaucomatous Eyes using Optical Coherence Tomography

Schuman J, Hee MR, Puliafito CA et al

Arch Ophthalmol. 1995; 113:586-596

This was the pilot study to quantitatively assess nerve fibre layer thickness in normal and glaucomatous eyes and correlate it with conventional measurements of optic nerve function by visual field examination. They studied 59 eyes of 33 subjects by Humphrey 24-2 visual fields, stereoscopic optic nerve head photography and optical coherence tomography. It showed a high degree of correlation between nerve fibre layer thickness measured by OCT and functional status of the optic nerve, assessed by visual field examination. Neither cupping of the optic nerve nor neuroretinal rim area where as strongly associated with visual field loss as was nerve fibre layer thickness.

Optical Coherence Tomography Measurement of Nerve Fibre Layer Thickness and the Likelihood of a Visual Field Defect

Williams ZY, Schuman JS, Gamell L et al

Am J Ophthalmol 2002; 134:538-546

Zinaria Y. Williams et al, in their publication tried to determine if optical coherence tomography measurements of nerve fibre layer thickness can be used to predict the presence of visual field defects associated with glaucoma. A retrospective study of OCT NFL thickness measurements in 276 eyes of 276 subjects was done; 136 eyes underwent frequency doubling technology perimetry and 140 eyes underwent Swedish Interactive threshold algorithm perimetry. They defined a parameter called $NFL_{50,}$ which is the NFL thickness value at which there is a 50% likelihood of a Visual Field Defect (VFD) with either SITA or FDT perimetry. They concluded that nerve fibre thickness analysis using OCT may be clinically useful in identifying subjects who have visual field loss.

Retinal Nerve Fibre Layer Thickness Measured with Optical Coherence Tomography is Related to Visual Function in Glaucomatous Eyes

El Beltagi TA, Bowd C, Boden C,et al

Ophthalmology 2003;110:2185-2191

Tarek A. El Beltagi et al studied the relationship between areas of glaucomatous retinal nerve fibre layer thinning by optical coherence tomography and areas of decreased visual field sensitivity identified by standard automated perimetry in glaucomatous eyes in their study published in 2003. They conducted a retrospective case study with 43 patients having glaucomatous optic neuropathy and imaged them with optical coherence tomography after automated perimetry. They concluded that localized retinal nerve fibre layer thinning, measured by optical coherence tomography is topographically related to decreased localized standard automated perimetry sensitivity in glaucoma patients. Also the retinal nerve fibre layer areas most frequently outside normal limits were the inferior and inferotemporal regions.

Evaluation of the glaucomatous damage on retinal nerve fibre layer thickness measured by optical coherence tomography

Kanamori A, Nakamura M, Escano MF, et al

Am J Ophthalmol. 2003;135:513-520

The study evaluated the relationship between visual field and retinal nerve fibre layer thickness measured by optical coherence tomography to assess the diagnostic ability of OCT to distinguish between early glaucomatous or glaucoma suspect eyes from normal eyes. A retrospective study on 160 eyes of 120 normal adults, 23 eyes of 16 patients with ocular hypertension, 38 eyes of

35 glaucoma suspect patients and 237 glaucomatous eyes of 140 glaucoma patients was done. Thickness of RNFL around the optic disc was determined with three 3.4 mm diameter circle OCT scans. Receiver operating characteristic curve area was calculated to discriminate normal eyes from early glaucomatous or glaucoma suspect eyes. A significant relationship existed between the mean deviation and RNFL thickness in all parameters excluding the 3-o' clock area.

Retinal Nerve Fibre Layer Measurement by Optical Coherence Tomography in glaucoma suspects with short-wavelength perimetry abnormalities

Mok KH, Lee VW, So KF et al

J Glaucoma. 2003;12:45-49

The study recruited 48 eyes of normal subjects, 34 eyes of glaucoma suspects with SWAP abnormalities and 38 eyes of early chronic primary open angle glaucoma subjects. All underwent normal conventional automated perimetry visual fields followed by OCT RNFL measurements. It concluded that compared with normal controls, OCT RNFL thickness was significantly lower in glaucoma suspects with abnormal SWAP and POAG patients, and this may aid in detection of glaucomatous damage earlier than standard conventional automated perimetry.

Optical Coherence Tomography Macular and Peripapillary Retinal Nerve Fibre Layer Measurements and Automated Visual Fields.

Wollstein G, Schuman JS, Price LL, et al

Am J Ophthalmol 2004;138:218-225

In a retrospective study 150 eyes from 101 subjects from a glaucoma series underwent Visual field testing by Humphrey full threshold 24-2 achromatic perimetry or Swedish Interactive Thresholding Algorithm (SITA) standard and OCT scans to assess peripapillary NFL data and Macular retinal thickness. Area under the receiver operator characteristics (AROC) curves for the association between macular retinal thickness and peripapillary NFL thickness and visual field findings were calculated in a subgroup of eyes without visual field defect and eyes with visual field defect confined to one hemifield. Macular retinal thickness was capable of determining glaucomatous damage and corresponded with peripapillary NFL thickness; however, peripapillary NFL thickness had higher sensitivity and specificity for the detection of visual field abnormalities.

IMAGING OF THE OPTIC NERVE AND NERVE FIBRE LAYER IN GLAUCOMA

The optic nerve was not visualized in living subjects routinely until Hermann von Helmholtz elaborated his ophthalmoscope in 1851[25]. Developments in automated and static perimetry have improved the accuracy and reproducibility of documenting visual field defects but patients may lose significant neural tissue prior to the development of detectable visual field loss[5]. Therefore, the appearance of the optic nerve and the adjacent nerve fibre layer are the best signs of glaucoma's presence or progression.

Subjective assessments of the Optic nerve head (ONH) cupping are not sufficiently sensitive to detect small changes, especially notches and other local abnormalities, and are unable to discriminate between glaucomatous and normal optic nerve head[26]. Drawings of the ONH and stereoscopic ONH photography, although useful clinical tools, depend on the subjective interpretation of the examiner and are thereby subject to variability in interpretation. Fundus photography was introduced with the development of the Nordenson camera, in the early twentieth century. Stereo optic disc photos have been used to document changes in the optic nerve appearance over time. Nerve fibre bundles have been demonstrated with the use of red free light. In addition, fluorescein angiography has been used to show areas of the optic disc.

Although photographs supply a true picture of the ONH at a point in time, their interpretation is extremely subjective[27]. Technology has been introduced over the past two decades to improve the examination of the ONH, and more recently, the NFL.

OPTIC NERVE HEAD ANALYSIS

PAR IS 2000/ Topcon IMAGEnet

Optic nerve head analyzers were developed to quantitate cupping, to measure ONH rim area and to provide other indices of ONH structure. Like fundus cameras, automated systems used standard fundus cameras optics and could digitize simultaneous stereo images either directly or from 35 mm slides[28]. By using algorithms for image registration and cross-correlation to calculate depth values at well matched corresponding points, a three dimensional map was created of the ONH.

Humphrey Retinal Analyzer

The Humphrey Retinal Analyzer used a familiar system but input was from a red free stereoscopic video camera[29].

Rodenstock Optic Nerve Head Analyzer

It used a method similar to the PAR instrument, the digital input coming directly from a stereoscopic video camera, and was obtained while projecting two sets of seven evenly spaced lines on the ONH[30].

The Glaucoma-Scope

The Glaucoma-scope is based on the principle of raster stereography. This instrument assesses the deviation of projected lines on the ONH to reconstruct three dimensional anatomy from a monocular image. It projects 25 parallel horizontal lines onto the ONH at an angle of 90° to the ONH surface, using an infrared light source[31, 32, and 33]. The lines are deflected proportionately to the depth of the surface. The images are recorded on a video monitor and the deflections are translated into depth values from approximately 8750 data points. A reference surface is used and is calculated from extrapolation of the data from two vertical lines 350 μm on either side of the ONH.

Unfortunately, optic nerve head analyzers cannot reliably differentiate between normal and glaucomatous optic nerve heads and are limited in their ability to detect change over time[12, 9, 13, 7, 10, 34-37]. Although these systems are an attempt to automate and thus increase the objectivity of optic nerve evaluation, their accuracy and reproducibility are still limited by the optics of the systems and they still rely a great deal on human control and interpretation.

LASER SCANNING OPHTHALMOSCOPY

Compared to the ONH analyzers, improved axial resolution and reduced variability in assessing optic nerve topography is achieved with the confocal scanning laser ophthalmoscopes, which produces optical sections of the retina

and ONH in a coronal plane. Scanning systems can be divided into two different categories based on the way that they detect the signal reflected back from the scanned object: confocal and non confocal.

Nonconfocal systems

In this system, a laser beam from a helium-neon, argon or infrared laser illuminates the eye. The beam is focused by the cornea onto the retina with a spot size of approximately 10 to 20 µm. The optical quality of the eye limits the minimum spot diameter. The laser beam is deflected by a rotating polygon for fast horizontal scanning and a galvanometer for slow vertical scanning to probe the fundus point by point and line by line. A partially reflective mirror separates the light backscattered from the retina and the illumination beam light. The detector receives a time-resolved image signal which is displayed on a video monitor[38, 39].

A scanning imaging system is advantageous because contrast is high due to selective illumination. At any given time only the point of the retina that is to be imaged is illuminated by the laser beam.

Confocal systems

The newer scanning laser ophthalmoscopes use a double scanning confocal optical system[40]. That is, the illuminating laser light is scanned across the retina along with the detector system. These confocal scanning microscopes are based on the principle of spot illumination and spot detection[41, 42, 43]. With

this type of imaging, only one spot on the retina is illuminated at a time through a pinhole aperture. A second small confocal aperture allows only light originating from the illuminated retinal area to pass through. The contrast is enhanced more than with nonconfocal scanning systems. Because the depth of field is dependent on the size of the detection aperture, depth of field can be varied by altering aperture diameter. When depth of field is reduced, layer by layer imaging is possible within the retina.

The Rodenstock Confocal Scanning Laser Ophthalmoscope

The Rodenstock Confocal Scanning Laser Ophthalmoscope (CSLO) obtains each focal plane image in one thirtieth of a second as a 525 horizontal line analog video signal with a field of view of 20 to 40 degrees and has a focal plane half-width thickness of 300 μm[40, 38].

Resolution with this system is dependent on laser spot size and imaging pinhole diameter rather than the optics of a fundus camera. The vertical resolution of depth is related to the spacing of the focal plane images. Although the scanning laser ophthalmoscope predominantly has served the purpose of imaging, the laser scanning tomographers provides and added feature of 3-dimensional measurements of ocular structures with good reproducibility[44].

The Heidelberg Laser Tomographic Scanner

The Heidelberg Laser Tomographic Scanner (LTS) used a helium neon laser beam focused onto the fundus[45]. Images with sizes up to 20 by 20 degrees

were obtained by scanning the structure point wise line by line in the given focal plane. In the case of optic disc recording, the first focal plane was defined directly above the first reflections of the retina. The last focal plane was selected in the region of the bottom of the excavation below the position of maximum reflectivity of the excavation. Within the preselected focal planes, the LTS automatically completed an optic disc scan of 32 consecutive focal plane sections from the preretinal plane to the bottom of the excavation[45]. Given the optical quality of the human eye, the depth resolution was 300 μm. Automatic compilation of an optic disc scan of 32 consecutive focal plane sections is done in about 4 seconds.

Compared to the ONH analyzers, improved axial resolution and reduced variability in assessing optic nerve topography is improved with confocal scanning laser ophthalmoscopes, which produce optical sections of the retina and the ONH in a coronal plane. Cross-sectional imaging of the fundus with scanning laser ophthalmoscopes and tomographs is limited by ocular aberrations and numerical aperture available through pupil to 300 μm axial resolution. A major disadvantage of CSLO ONH measurements is that a reference plane is required to measure and calculate many of the parameters. The current software of the HRT defines the "standard reference plane" as a plane 50 μm posterior to the mean height of the peripapillary retinal height along the contour line at a temporal segment between 350° and 356° below the

horizontal line. Therefore the reference plane may change over time and give inaccurate data, especially in those with glaucoma who have changing topography[46]. Parameters that are independent of the reference plane include cup shape, cup volume below the surface, mean cup depth, maximum cup depth, and disc area.

ONH analyzers developed to quantitate cupping can measure rim area and provide indices of structure, but cannot as yet differentiate between normal and glaucomatous nerve heads and can only make limited efforts to detect changes over time.

NERVE FIBRE LAYER ANALYSIS

Studies of the NFL, rather than the optic nerve, should be used to detect the earliest signs of glaucomatous damage. Quigley and co-workers showed that change in retinal thickness due to NFL thinning secondary to ganglion cell death is a sensitive indicator of glaucomatous damage and may precede detectable changes in ONH appearance (cupping) and measurable loss of visual functions[47, 48, 49]. A reduction in thickness of only 10 to 20 μm may be significant, indicating impending visual field loss[47]. In fact, it is ganglion cell death that produces visual loss in glaucoma, and changes in the ONH only reflect the atrophy of the ganglion cells.

The nerve fibre analyzer

The NFL has birefringent properties: back and forth travel of light through it causes a change of polarization known as retardance. Polarized light propagating through the retina is assumed to be rotated by the NFL in proportion to its thickness; therefore, measurements of the polarization state of reflected light provide information on NFL thickness. NFL thickness can be evaluated by measuring the retardance using Fourier ellipsometry[50].

Scanning laser ophthalmoscope

The high visibility of the NFL resulting from the high contrast imaging inherent in the confocal laser scanning configuration can be further enhanced using digital image enhancement techniques[51, 52]. The confocal microscope can image NFL striations with high contrast and high lateral resolution and is not as dependent on pupil dilation or clear media as traditional photographic techniques[53]. The NFL striations are enhanced in this approach using digital filtering and polarization differential contrast imaging, in which changes in NFL appearance due to NFL birefringence are evaluated using two images obtained simultaneously with orthogonal polarization[54].

Scanning laser polarimetry

Scanning laser polarimetry (NFA, NFA II, GDx) is a method of measuring the retinal nerve fibre layer thickness by use of a 780 nm near infrared diode polarized light. The double-passed reflected light is detected and

analyzed in digital form and after adjacent scans are achieved, displayed in the form of a 256 x 256 pixel representing individual retinal positions covering 15°. The value of each pixel represents the amount of retardation – qualitatively yellow and white for high retardances while those that are dark blue represent low retardation. The time to acquire these 65,536 data locations is approximately 0.7 seconds. Measurements are obtained from a circular band of 1.5 to 2.5 disc diameters concentric to the disc. During the time of measurement, a compensation device neutralizes the corneal birefringence (but not the lenticular birefringence) to maximize polarization measurements of the retina[56].

An advantage of the scanning laser polarimeter is that it does not require pupil dilation. The polarimeter seems to be unaffected by both contact lens wear from +4.0 dioptres to -8.5 dioptres and excimer laser treatment of corneas for moderate myopia. One disadvantage of the polarimeter is that the cornea and lens are polarizing structures that may alter the retardance, even with the use of the corneal compensator. In addition, retardance is a relative value and does not produce absolute NFL thickness values, unlike HRT and OCT measurements.

RETINAL THICKNESS MAPPING

Retinal thickness mapping with the Retinal Thickness Analyzer (RTA) is based on the principle of slit-lamp biomicroscopy in which a green 540 nm HeNe laser is projected on the fundus at an angle and its intersection with the retina is imaged. The distance between the intersection with the vitreo-retinal interface and that with the retina-retinal pigment epithelial interface is directly proportional to the retinal thickness. In about 400 ms, a 2 x 2 mm area of the fundus is scanned, yielding 10 optical cross sections that are digitally recorded and an algorithm detects points grossly deviating from their neighbours. Unlike OCT, which yields individual optic sections, the retinal thickness mapping is capable of rapidly covering the macular area and its location relative to the fovea. The RTA is limited by pupil size and it is difficult to image those eyes with numerous floaters or media opacities such as advanced cortical cataracts[55].

CONFOCAL TOMOGRAPHIC ANGIOGRAPHY

This system combines the confocal laser scanner and Indocyanine green to visualize the vascular pattern of the deeper portions of the ONH, including the lamina cribrosa. Studies have proven that confocal tomographic angiography of patients with glaucomatous eyes had good correlation with their visual field defect location[56].

NEW OBJECTIVE FUNCTIONAL TESTS

All of the prior technologies to image the optic disc and NFL in glaucoma have been based on structural testing. Perimetry is a functional test that correlated well with structural assessments but is a subjective test that may not be able to detect early glaucomatous changes. Other functional tests showing promises are the pattern electroretinography (PERG) and multifocal electroretinography (MFERG) [56].

OPTICAL COHERENCE TOMOGRAPHY

The traditional view of the fundus provided by the ophthalmoscope is limited. Direct cross-sectional imaging of the retinal anatomy could benefit the early diagnosis and more sensitive monitoring of a variety of retinal and optic nerve head diseases, such as glaucoma. Current techniques for ocular imaging do not have sufficient depth resolution in the posterior segment of the eye to provide useful cross-sectional images of retinal structure. The resolution of ultrasound is limited by the acoustic wavelength in ocular tissue to about 150 μm[58, 59]. High-frequency ultrasound increases the resolution to about 20 μm but cannot be applied to the posterior segment owing to limited penetration[60]. The resolution of computed tomography and magnetic resonance imaging is also limited to hundreds of microns[61, 62]. Cross-sectional imaging of the fundus with scanning laser ophthalmoscopy[63] and scanning laser tomography[64] is limited by ocular aberrations and the numerical aperture available through the pupil, to about 300 μm[64]. The optical coherence tomography is a relatively new imaging modality that involves the use of a 'low-coherence continuous-wave' light source and 'interferometry'. Cross-sectional information concerning retinal topography and internal tissue structure is obtained with 10 μm of longitudinal resolution from the time delay of reflected light using low-coherence interferometry[65]. **(Figure 1)**
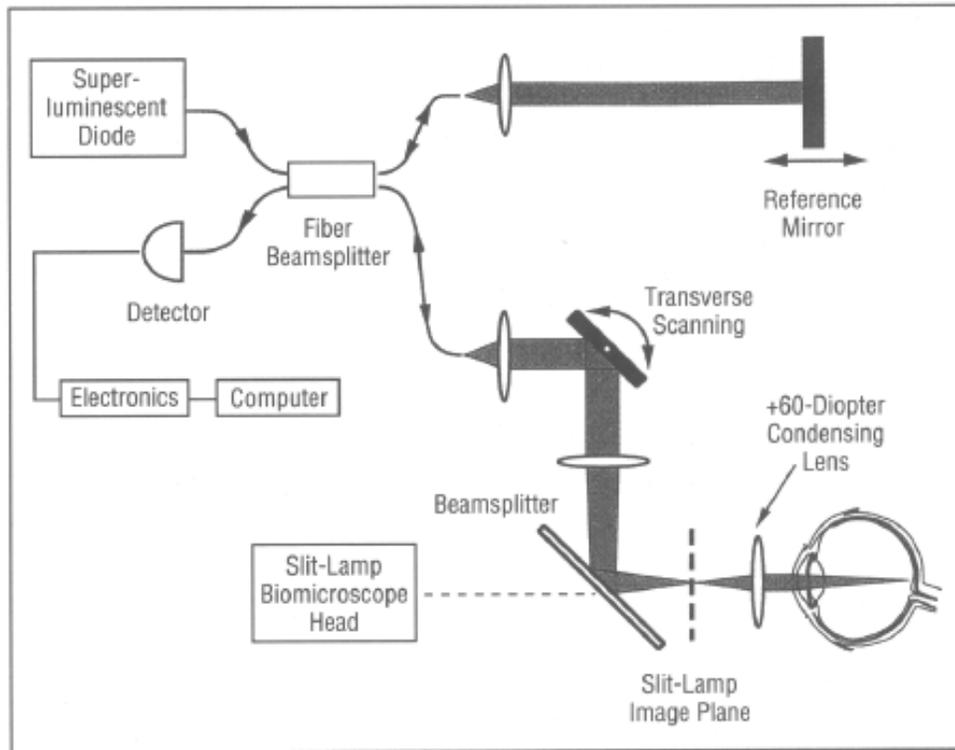
Figure 1. *Schematic diagram of the fiberoptic interferometer and imaging optics comprising the optical coherence tomographic scanner. Cross-sectional images of optical reflectivity vs depth are created in a manner similar to ultrasound B scan. The axial resolution is determined by the coherence length of the superluminescent diode source and is 10 μm (full width at half-maximum) in the retina.*

Low-coherence light from a superluminescent diode source is coupled into a fibreoptic Michelson interferometer. Infrared light at 843 nm is divided at a fibre coupler into reference and sample paths. Light retro reflected from a variable distance reference mirror is recombined in the coupler with light backscattered from the subject's eye. Temporal information is contained in the interference signal between the reference and sample beams, which is detected

by a photodiode followed by signal-processing electronics and computer data acquisition. With 175 µW of power incident on the eye, the system is sensitive to weakly reflected light as small as 50 femtowatts.

A longitudinal profile of reflectivity vs. depth into the sample similar to an ultrasound A-scan is obtained by rapidly translating the reference arm mirror and synchronously recording the magnitude of the resulting interference signal, which is evident only when the reference arm distance matches the length of a reflective path through the eye to within the source coherence length. The superluminescent diode has a coherence length in the eye of 10 µm full width at half-maximum that defines the longitudinal ranging resolution and is unaffected by ocular aberrations or the limited pupil diameter. In analogy to ultrasound B mode, cross-sectional images are constructed from a sequence of single longitudinal reflectivity profiles obtained by repetitively translating the reference mirror while scanning the probe beam across the retina. A typical B-scan OCT of the retina containing 100 longitudinal A scans is acquired in 2.5 seconds. The minimum lateral image resolution is determined by the beam waist diameter in the eye. The scanning beam diameter at the cornea is 1.2 mm which, neglecting ocular aberrations, results in an estimated 13 µm (full width at half-maximum) spot size on the retina using Gullstrand's reduced schematic eye. The OCT scanning and imaging optics are retrofitted onto a standard slit-lamp biomicroscope. Two orthogonally mounted scanning mirrors provide

lateral beam positioning on the retina. Retinal tomography is performed in a manner similar to indirect ophthalmoscopy, whereby a +60 dioptre (D) double aspheric condensing lens mounted on the slit lamp in front of the eye is used to relay an image of the retina onto the slit-lamp image plane. Computer control and data acquisition enable a selection of a wide range of scanning patterns on the fundus and provide a real-time display of the tomography in progress. An infrared-sensitive charge coupled device video camera attached to the slit lamp provides a video image of the scanning OCT probe beam on the fundus and permits the position of each tomography on the retina to be documented **(Figure 2)**. Alternatively, direct slit-lamp observation of the fundus and probe beam may be performed using a visible aiming laser that is coupled into the OCT system and provides a visible spot coincident with the infrared probe beam on the retina[65].

OCT EXAMINATION PROTOCAL

The retinal examination with OCT is performed in a manner similar to slit-lamp indirect ophthalmoscopy, with the restriction that the condensing lens is mounted and fixed along the slit-lamp optical axis. After the eye is dilated and the patient is positioned comfortably in the slit-lamp headrest, the slit lamp and the condensing lens unit are positioned along the optical axis of the eye. The entire unit is brought forward until the imaging lens is about 1cm from the

eye placing an image of the fundus is brought into focus. This adjustment compensates for differences in the refractive power between patients without being affected by accommodation in the examiner's eye. The desired scanning position is then located while the examiner observes both the real-time display of the OCT in progress and the direct or video image of the OCT probe beam location on the fundus. The +60 D condensing lens provides a field of view of approximately 25º, which is sufficient for tomographs encompassing either, the macular or peripapillary region. Higher or lower-power condensing lenses may be interchanged to achieve either a wider field of view or higher magnification, respectively **(Figure 3)**. The OCT examination may also be performed with an undilated or poorly dilated pupil; however, the optical alignment is more sensitive to aperturing by the pupil and the field of view is reduced.

Since the condensing lens is fixed to the slit lamp, different regions of the retina are imaged by translating the subject's fixation point, rather than by altering the position of the slit lamp. To allow precise positioning on the retina, a fixation spot is generated under computer control by the OCT probe beam that is interleaved with the scanning pattern on the retina of the eye being imaged. Fine positioning of OCT scan is achieved by directly adjusting the position of the scanning probe beam under computer control[65].

INTERPRETATION OF THE OCT

OCT differentiates between light backscattered from different depths in the retina, permitting characterization of internal retinal structure. A highly reflective red layer delineates the posterior boundary of the retina in the tomograph and probably corresponds to the retinal pigment epithelium and choriocapillaries. This posterior layer terminates at the margin of the optic disc consistent with the termination of choroidal circulation at the lamina cribrosa. Below the choriocapillaries, relatively weak reflections are observed from the deep choroid and sclera, due to attenuation of the signal passing through the retina. A dark layer indicative of minimal reflectivity appears just anterior to the choriocapillaries and pigment epithelium and probably represents the outer segments of the retinal photoreceptors. The intermediate layers of the retina anterior to these segments exhibit moderate backscattering. According to the tomograph, the RNFL increases in thickness from the macula to the optic disc as expected from normal anatomy. The reflectance from the RNFL decreases in the region of the optic disc[65].

OCT FOR IMAGING THE OPTIC DISC

For imaging the optic disc, peripapillary regions, and retinal nerve fibre layer, two types of scans are used: radial sections at different orientations each passing through the centre of the disc, and tomographs taken while scanning the

probe beam circularly around the disc. Each 100(horizontal) x (250 vertical) pixel image was acquired in 2.5 seconds and corresponds to a 6.75 mm radial slice through the nerve head **(Figure 4)**. The location of each tomograph on the retina is labelled on the fundus photograph. In the 90º tomograph (taken perpendicular to the papillomacular axis), high backscattering (red) is visible from two prominent layers that probably correspond to the RNFL and choriocapillaris **(Figure 5)**. The tomograph shows the RNFL expanding toward the optic disc to occupy nearly the entire retinal thickness, commensurate with the presence of the inferior and superior arcuate nerve fibre bundles. In comparison, the 0º tomograph (taken parallel to the papillomacular axis) exhibits a thinner RNFL consistent with less well-defined fibre bundles[65].

OCT FOR RETINAL THICKNESS MEASUREMENT

Measurements of retinal and RNFL thickness are potentially important for the diagnosis and treatment of diseases such as macular degeneration, macular edema and glaucoma. A computer program estimates the retinal thickness for the OCT scan in the image as the distance between the vitreoretinal interface and the anterior boundary of the retinal pigment epithelium and choriocapillaries. The location of these boundaries was determined by a simple thresholding algorithm that searched for the change in reflectivity evident at each of these interfaces. In a similar manner, the

thickness of the RNFL was also estimated by computer and was assumed to be correlated with the extent of the red, highly reflective layer at the inner margin of the retina. The Mean + S.D. for the thickness measurements were $230\pm15\mu m$ and $90\pm18\mu m$ for the retina and putative RNFL, respectively.

OCT – CIRCULAR TOMOGRAPHS IN THE PERIPAPILLARY REGION

Variations in retinal and RNFL thickness are most striking in the peripapillary region, where bundling of nerve fibres creates distinct anatomic variations in the thickness. Documentation of nerve fibre layer thickness and degeneration in this region is also important in the diagnosis and treatment of glaucoma. OCT is used to cross sectionally image the retina in cylindrical sections of tissue surrounding the optic nerve head. Two circular OCTs with different diameters, each centred on the nerve head are taken. Each 100 (horizontal) x 250 (vertical) pixel tomography is displayed unwrapped and corresponds to a counter clockwise scan around the optic disc. The inferotemporal and superotemporal nerve fibre bundles are evident in both tomographs as localized thickenings in both the RNFL and retina. In the 1.5 disc diameter circular tomography, the retinal thickness varies between 220 μm nasally to 400 μm in the superotemporal bundle, while the RNFL thickness correspondingly varies between 40 μm and 230 μm. In the 2 disc diameter

image, both the retinal and RNFL are generally thinner owing to the increased distance from the nerve head margin. The retinal thickness reaches a minimum of 200μm nasally and a maximum of 310μm superotemporally, while the RNFL thickness varies between 30μm and 190 μm.

OCT IN GLAUCOMA

The STRAUS OCT ^{TM} 3 was used for this study and STRAUS OCT software 2.0 for analysis. The Retinal nerve fibre analysis uses three 1.73 mm radius line scans centred on the cup. The optic nerve head analysis uses six 4 mm radial line scans centred on the cup. Macular analysis uses six 4mm radial line scans centred on the fovea.

The nerve fibre layer thickness is colour coded according to the age related normal of the population. 95% of normal population falls in or below green band and 90% falls within green band. 5% of normal population falls within or below yellow band. 1% falls within red band and is considered outside normal limits **(Figure 6)**.

The average RNFL thickness in normal and disease conditions (Schuman et al, Ophthalmol, 2003):

- ➢ Normal   95.9±11.4
- ➢ Early glaucoma   80.3 ± 18.4
- ➢ Advanced glaucoma 50.7 ±13.6

Mean RNFL thickness (Results of OCT from the AEH study)

244 eyes of 122 normal subjects were studied of which 64 (52.5%) were male and 58(47.5%) were female. The mean age of the subjects were 44.25±13.95 years (range 21-74 years)

	Mean ±S.D.
Superior	140.22± 21.17
Nasal	88.59± 21.16
Inferior	125.34± 19.71
Temporal	66.62 ±15.9
Average	**104.97 ±15.14**

Bilateral comparison of both eyes is possible with OCT enabling the analysis of the symmetry between the right and left eyes. Asymmetry in RNFL can be picked up as a sensitive indicator of glaucomatous loss. OCT also enables serial analysis to manage the disease and follow progression of glaucomatous damage. The software package allows analysis simultaneously of as many as four right and four left scans.

The Optic nerve head scanning takes six radial scans and gives the following data

- Disk area (normal 2.139mm2)

- Cup area (normal 0.775mm2)

- Rim area (normal 1.364mm2)

- Cup/ Disc ratio

  -Horizontal

  -Vertical

The ONH scan objectively locates the optic disc using signal reflected from the Retinal pigment epithelium and provides volumetric and area analysis of the optic cup, optic disc and neuroretinal rim. The precise automated measurement eliminates any operator subjectivity and gives accurate cup/disc ratios.

VISUAL FIELD ANALYSIS – HUMPHREY FIELD ANALYSER

Two steps are involved in diagnosing glaucomatous visual field loss using automated perimetry. The first is to determine whether or not the visual field is normal. If the visual field is abnormal, the second step is to decide if the visual field abnormality is due to glaucoma or something else. When applied to perimetry, the term normal actually describes the range of test results found in the nondiseased population. The range of normal has been determined experimentally, and the results are stored in the computer memory of the automated perimeter. If all statistical parameters are within the normal range, chances are that the visual field is normal. The sensitivity of automated threshold perimetry for detecting visual field defects is very high. But the specificity of automated perimetry is often not as high as clinicians would like. When performing perimetry on patients believed to have glaucoma, it is important to distinguish the visual field that appears abnormal because of artefacts from the visual field that are truly abnormal as a result of glaucoma or some other disease such as cataract, retinal disease, or neurologic lesions[66].

RELIABILITY INDICES

Reliability is tested by presenting "catch trial" targets designed to measure fixation losses, false-positive responses, and false-negative responses.

The fixation loss rate relates to the number of times a patient responds to a target placed in the blind spot. If the fixation loss rate exceeds 20%, it is flagged. The false-positive error rate refers to the number of times a patient responds to the audible click of the perimeter's shutter when no target is presented. The false-negative error rate refers to the number of times a patient fails to respond to a suprathreshold (very bright) target placed in a seeing area of the visual field. The false-positive and false-negative errors are flagged if either exceeds 33%. The reliability indices are indicators of the extent to which a particular patient's results may be reliable compared with the normal range of values stored in the computer memory[67-69].

The patient's visual sensitivity for the fovea appears immediately below the reliability indices, along with any symbols denoting if foveal threshold fall beyond the normal 5%, 2%, 1% or 0.5% probability levels. The patient's visual sensitivity at each field location is presented below and to the right of the foveal sensitivity, with numeric values on the left and a graphic grey scale representation on the right. The numeric display gives the sensitivity of the visual field in decibels, with higher numbers denoting greater sensitivity. Decibels are a logarithmically based scale (10dB = 1 log unit) and represent units of attenuation of the highest luminance stimulus that the perimeter can present[66].

GREY SCALE

The grey scale indicates areas of high sensitivity with light shading and progressively lower sensitivities with darker shadings and so provides the reader with an overview of the pattern of visual field sensitivity. Given that this representation is based upon sampling locations within the visual field, the grey scale "fills in" areas between these tested locations by interpolation[66].

GLOBAL INDICES

The four global indices are found in the lower right hand corner of the printout. The mean deviation (MD) is a measure of the average departure of each test location from the age-corrected normal value. The pattern standard deviation (PSD) is the standard deviation of the differences between the threshold value at each test location and the expected value. It is a measure of the extent to which the threshold determinations differ from each other. The short term fluctuation (SF) represents the variability of the patient's responses during the test. The corrected pattern standard deviation (CPSD) is similar to the PSD but is adjusted downward by subtracting that portion of the PSD which is actually caused by the SF. The calculation of global indices is weighted to give greater importance to the test locations near fixation and less importance to more peripheral locations[69, 70, 71].

If a global index is outside the expected normal range, a "P" value will appear next to it. The P value represents the proportion of normal subjects in which an index of that value is found. For example, if P < 1% appears next to MD, fewer than 1% of normal subjects of that age will have an MD at that level. Any global index with a P value less than 5% has a high probability of being abnormal.

The MD is mainly an index of the size of a visual field defect. The MD is very sensitive to generalized loss of sensitivity, but purely localized defects that are large enough will also affect the MD.

The CPSD is an index of localized nonuniformity of the surface of the hill of vision. It is extremely sensitive to localized visual field defects and is not at all affected by purely generalized loss of sensitivity. By looking at the MD and the CPSD, it is possible to anticipate the nature of any visual field defect before inspecting the rest of the data.

Table 1. Interpretation of the global indices on the Humphrey visual field analyzer

MD	CPSD	Interpretation
Normal	Normal	Visual field probably normal
Abnormal	Normal	Generalized loss of sensitivity
Normal	Abnormal	Small localized defect
Abnormal	Abnormal	Large defect with a significant localized component

TOTAL AND PATTERN DEVIATION

The total and pattern deviations are arrays of numbers and graphic plots in the centre and lower portions of the printout. The total deviation represents the difference between the measured threshold of each individual test location and the age-corrected normal value for that location. Visual field thresholds decline with age at the rate of between 0.5 and 1.0 decibels per decade. The pattern deviation represents the difference between an adjusted threshold of each individual test location and the age-corrected normal value for that location. The pattern deviation is derived from the total deviation by adjusting the measured thresholds upward or downward by an amount that reflects any generalized change in the threshold of the least damaged portion of the visual field.

The graphic probability plots indicate how frequently a total or pattern deviation value at a particular test location will be found in the normal population. There are four symbols ranging from P<5% to P<0.5%[66].

GLAUCOMA HEMIFIELD TEST

The Glaucoma Hemifield test attempts to provide information about the difference between the superior and inferior halves of the visual field[72, 73]. The test evaluates the differences in threshold of mirror image groups of points on either side of the horizontal midline. There are five interpretive messages that

may appear depending on the relationship of the thresholds in the superior and inferior halves of the field.

1. Within Normal Limits means that there is no significant difference between the superior and inferior halves of the fields and the overall sensitivity is within the 99.5% range of normal.

2. Outside Normal Limits appears when the threshold differences between the groups of points compared in the superior and inferior halves of the field are greater than would be expected in 99% of the normal population.

3. Borderline appears when the threshold differences are greater than would be expected in 97% of the normal population but not as great as in Outside Normal Limits.

4. General Reduction of Sensitivity appears when the overall sensitivity of the least damaged portion of the visual field is depressed below the 99.5% range of normal, but there is no significant difference between the superior and inferior halves of the field.

5. Abnormally High Sensitivity appears when the overall sensitivity is higher than expected in 99.5% of the normal population. This message is found most often in the presence of a high false-positive rate and usually represents an artefact of testing.

The specificity and sensitivity of the Glaucoma Hemifield Test for detecting nerve fibre bundle visual field defects are quite high.

CHOICE OF TEST PROGRAM

The standard test program used in glaucoma patients is the 30-2. The 24-2 eliminates the peripheral test locations of the 30-2 program except for the most nasal portion of the field. The 10-2 program is useful in patients with very advanced field loss who only have a small island of vision persisting near fixation. The foveal sensitivity is also a very useful piece of information and should be turned on when performing threshold perimetry in glaucoma patients. Either the full threshold or full threshold from prior data strategies should be used when performing perimetry on the Humphrey Visual Field Analyzer[66].

NATURE OF GLAUCOMATOUS VISUAL FIELD DEFECTS

NERVE FIBRE BUNDLE DEFECTS

Most visual field defects seen in glaucoma are of the nerve fibre bundle type[74]. Glaucoma causes loss of retinal fibre bundles by damaging ganglion cell axons at the optic nerve head. This loss may be either diffuse, localized, or both. The characteristic shape and location of the visual field defects seen in glaucoma result from the anatomy of the retinal nerve fibre layer[75]. The most characteristic feature of the nerve fibre bundle visual defect is the tendency to

respect the horizontal meridian, especially of the nasal portion of the field. Isolated nerve fibre bundle defects rarely cross the nasal horizontal midline and typically end there abruptly. Even in patients with more advanced visual loss due to glaucoma, a detectable difference in the measured threshold on either side of the nasal horizontal midline often occurs.

Another feature of nerve fibre bundle visual field defects is the tendency to be found in the Bjerrum area which is between 10° and 20° from fixation temporally but fans out to between 2° and 25° nasally. Scotomas in this area often assume an arcuate shape with the circumferential diameter greater than the radial diameter. Fixation itself is usually spared unless the defect is far advanced. Nerve fibre bundle defects may, however, come to within 1° of fixation.

Clinically, nerve fibre bundle defects may appear as paracentral or arcuate scotomas, nasal steps, temporal sector defects, or various combinations. Generalized loss of retinal sensitivity, enlargement of the blind spot, and selective loss of sensitivity in the nasal periphery without specific nerve fibre bundle characteristics have been described in glaucoma. There are many other causes for these types of visual field defects. Although any of them may occur as an isolated finding in glaucoma, more commonly they are associated with a nerve fibre bundle defect.

ARTEFACTS THAT MAY RESEMBLE VISUAL FIELD DEFECTS

Many artefacts of visual field testing can produce results resembling true visual field defects. An artefact does not reflect abnormal visual function. Rather, it results from the way the patient responds to the testing situation. Generalized depressions such as those seen in patients with cataracts or small pupils are not artefacts. They are true visual field defects that reflect diminished visual function. The learning effect is a common artefact in patients undergoing their first visual field examination. It typically appears as a loss of sensitivity which is more pronounced in the more peripheral portions of the field. The defect either disappears or markedly improves after the second or third examination. An apparent depression in the superior peripheral portion of the field may resemble an arcuate scotoma in the grey scale. The superior portion of the visual field normally has lower sensitivity and higher variability. Even mild blepharoptosis may produce significant depressions in the superior visual field resembling the defects seen in glaucoma. To obtain accurate central visual fields, the patient's refractive correction must be placed in the perimeter. In general, about one decibel of loss will appear for each dioptre of over or under correction placed in the perimeter. If the pupil is smaller than 2.5 mm, an otherwise normal visual field may appear to be depressed, whereas an abnormal visual field may appear worse than it really is[76]. The pupil size should be recorded each time the visual field is tested. Fatigue and an unduly long

examination time may also be associated with depressed sensitivity and apparent visual field defects[77].

In conclusion, automated perimetry is an extremely useful tool and has become the standard technique for evaluating the visual field in patients with or believed to have glaucoma. Interpretation of the results is difficult and requires experience as well as a detailed understanding of the underlying principles of automated static perimetry and applied statistical analysis. OCT nerve fibre analysis corresponds well with the visual field defects detected by standard automated perimetry. **(Figure 7)**.

AIMS AND OBJECTIVES

PURPOSE

To quantitatively assess the retinal peripapillary nerve fibre layer using optical coherence tomography and compare with standard automated perimetry in eyes with primary open angle glaucoma.

AIMS

- To quantitatively assess the retinal peripapillary nerve fibre layer in eyes with primary open glaucoma and evaluate its efficacy in diagnosing glaucoma

- To correlate the retinal nerve fibre layer thickness with a diagnostic gold standard, in this case standard automated perimetry by Humphrey's visual field analyser

- To compare the efficacy of each of these investigations in diagnosing primary open angle glaucoma.

- To investigate the agreement in glaucomatous damage detection between structural changes by OCT and functional alteration by automated perimetry.

MATERIALS AND METHODS

A prospective study to quantitatively measure the peripapillary retinal nerve fibre layer using optical coherence tomography and compare it with standard automated perimetry using Humphrey visual field analyser in patients with primary open angle glaucoma was undertaken in the Department of Glaucoma Services, Aravind Eye Hospitals, Madurai. The study was conducted for a period of two years from 1st July 2003 to 31st July 2005 during which time 76 eyes of 38 patients were studied and analysed.

SUBJECTS

INCLUSION CRITERIA

Best corrected visual acuity of at least 6/12 or better

Age < 60 years

Patients diagnosed with Primary open angle glaucoma at the time of diagnosis or after investigation

Open angles (angle grading >2 by Shaffer's system)

Patients cooperative for visual field analysis and OCT

Refractive errors

Myopia < -5D

Hypermetropia < +3.5D

Astigmatism < 2D

EXCLUSION CRITERIA

Age > 60 years of age

Closed angles by Gonioscopy

Media opacities – cataractous lenticular changes, vitreous haemorrhage, corneal edema/ opacity - which preclude examination of the posterior segment

Retinal pathology – advanced diabetic retinopathy, age related macular degeneration, retinitis pigmentosa, maculopathy.

All secondary glaucomas

All juvenile glaucomas

All subjects had a complete ophthalmologic examination including thorough slit lamp examination, Gonioscopy, dilated direct and indirect ophthalmoscopy, intra ocular pressure measurement using Goldmann Applanation tonometry, central corneal thickness measurement and refraction.

Glaucomatous eyes were designated on the basis of dilated fundus examination. Glaucomatous appearance of the optic disc defined as thinning of the neuroretinal rim, disc haemorrhage, notch, excavation, an RNFL defect or asymmetry of vertical cup disc ratio of greater than 0.2 between the two eyes. Two independent investigators examined these eyes and designated them as having primary open angle glaucoma or not having primary open glaucoma. They were not shown the visual field analysis or the OCT data to avoid bias.

OPTICAL COHERENCE TOMOGRAPHY

The STRAUS OCT [TM] [3] was used for this study and STRAUS OCT software 2.0 for analysis. The Retinal nerve fibre analysis uses three 1.73 mm radius line scans centred on the cup. The optic nerve head analysis uses six 4 mm radial line scans centred on the cup.

The OCT software measures the retinal nerve fibre layer thickness and analyses it. The nerve fibre layer thickness is colour coded according to the age related normal of the population. 95% of normal population falls in or below green band and 90% falls within green band. 5% of normal population falls within or below yellow band. 1% falls within red band and is considered outside normal limits. Retinal nerve fibre layer thickness measurements were considered outside of normal limits if they were thinner than 97.5% of normal values derived from healthy eyes in the normative database of our clinic.

STANDARD AUTOMATED PERIMETRY

Standard automated perimetry was conducted by using the Humphrey Field Analyzer II 24-2 program (Carl Zeiss Meditec) with a Goldmann size III (0.43°) stimulus on a 31.5 apostilb background within 6 months of OCT testing. All tests were reliable (with false positives, false negatives ≤33% and fixation losses ≤ 20%).

Glaucomatous visual field defect was defined as a cluster of 3 or more adjacent non-edge points depressed to an extent found in less than 5 % of population (i.e., P<5%) clustered in the arcuate area,

Pattern Standard Deviation depressed to an extent found in less than 5% of the population (i.e. P<5%)

An abnormal glaucoma hemifield test

PROFORMA

Optical Coherence Tomography and Visual Fields in Primary Open angle glaucoma Study

Name: Age: Sex:

Address:

M.R.No

Diagnosis:

OCULAR EXAMINATION

	Right eye	Left eye

VISUAL ACUITY

    Without correction

    With correction

PUPIL

    Size and shape

        1. Normal

        2. Altered

        3. Pseudoexfoliation

    Reaction to light

        1. Reacting briskly

        2. RAPD

        3. Sluggish

LENS

1. Clear

2. Cataract

3. Pseudoexfoliation

4. Subluxation/ Dislocation

INTRA OCULAR PRESSURE

(By Goldmann Applanation tonometry)

Time _____

FUNDUS

Vertical cup/ disc ratio

Notching/ Thinning of Neuroretinal rim

1. Absent

2. Superior Pole

3. Inferior Pole

Disc Haemorrhages

1. Absent

2. Present

Nerve Fibre Layer Defects

1. Absent

2. Inferior

3. Superior

4. Nasal

5. Temporal

VISUAL FIELD DEFECTS (By Humphrey's visual field analysis)

Field defects

1. Absent
2. Superior Arcuate Scotoma
3. Inferior Arcuate Scotoma
4. Nasal Step
5. Double Arcuate Scotoma
6. Paracentral Scotoma
7. Generalized Reduction of Sensitivity

Mean deviation

Pattern mean standard deviation

CENTRAL CORNEAL THICKNESS

OPTICAL COHERENCE TOMOGRAPHY

	OD	OS
Smax		
Imax		
Average Thickness		

OBSERVATIONS

About The Receiver Operating Characteristic curve

Sensitivity and specificity are the basic measures of accuracy of a diagnostic test. They describe the abilities of a test to enable one to correctly diagnose disease when disease is actually present and to correctly rule out disease when it is truly absent.

However, they depend on the cut point used to define "positive" and "negative" test results. As the cut point shifts, sensitivity and specificity shift. The receiver operating characteristic (ROC) curve is a plot of the sensitivity of a test (plotted on the y-axis) versus its false-positive rate (1-specificity, plotted on the x-axis) for all possible cut points.

The accuracy of a test is measured by comparing the results of the test to the true disease status of the patient. The true disease status is determined with the reference standard procedure[78].

The ROC curve area is a good summary measure of test accuracy because it does not depend on the prevalence of the disease or the cut points used to form the curve. The ROC curve has been used to assess the test accuracy of OCT and Visual Fields in diagnosing Glaucoma.

An ROC curve demonstrates several things:

1. It shows the tradeoff between sensitivity and specificity (any increase in sensitivity will be accompanied by a decrease in specificity).

2. The closer the curve follows the left-hand border and then the top border of the ROC space, the more accurate the test.

3. The closer the curve comes to the 45-degree diagonal of the ROC space, the less accurate the test.

4. The slope of the tangent line at a cut point gives the likelihood ratio (LR) for that value of the test.

5. The area under the curve (AUC) is a measure of test accuracy.

Chart 1 : Area under the receiver operator characteristic curve for optical coherence tomography peripapillary NFL measurements for eyes with primary open angle glaucoma
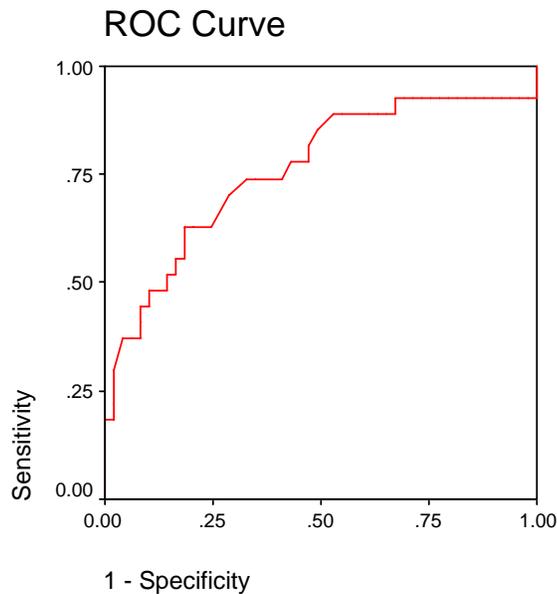
ROC Curve

Area Under the Curve

Test Result Variable(s): OCT

Area	Std. Error[a]	Asymptotic Sig.[b]	Asymptotic 95% Confidence Interval	
			Lower Bound	Upper Bound
.761	.062	.000	.640	.882

The test result variable(s): OCT has at least one tie between the positive actual state group and the negative actual state group. Statistics may be biased.

a. Under the nonparametric assumption

b. Null hypothesis: true area = 0.5

The area under the curve (AUC) is significant to state the test (OCT peripapillary NFL measurement) is accurate to diagnose the disease (Primary open angle glaucoma)

Chart 2 : Area under the receiver operator characteristic curves for OCT peripapillary NFL measurements in patients with Visual Field Defects by Humphrey's field analysis
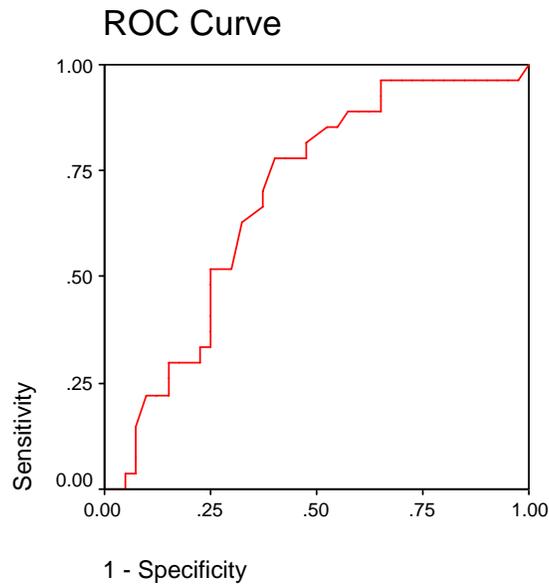
ROC Curve

Area Under the Curve

Test Result Variable(s): OCT

Area	Std. Error[a]	Asymptotic Sig.[b]	Asymptotic 95% Confidence Interval	
			Lower Bound	Upper Bound
.686	.066	.010	.557	.814

The test result variable(s): OCT has at least one tie between the positive actual state group and the negative actual state group. Statistics may be biased.

a. Under the nonparametric assumption

b. Null hypothesis: true area = 0.5

The AUC is fairly significant enough to state that the diagnostic modality being tested (OCT peripapillary NFL measurement) is comparable with the standard diagnostic modality for diagnosing the disease (Standard automated perimetry - Humphrey's visual field analyser).

Chart 3 : Area under the receiver operator characteristic curve for OCT superior peripapillary NFL measurements in patients with inferior hemifield visual defects

ROC Curve
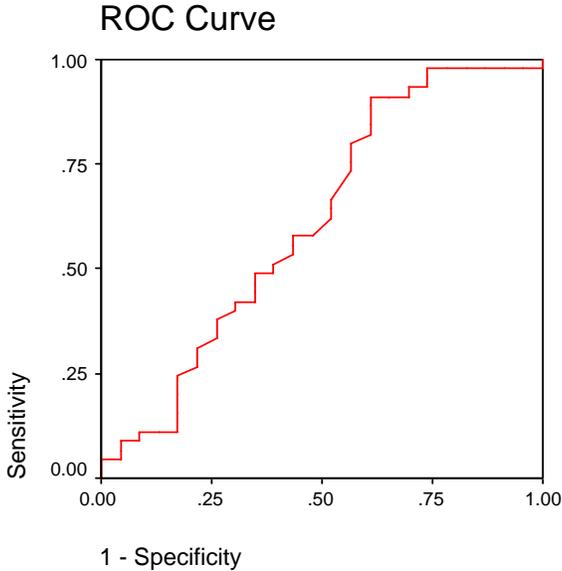
Area Under the Curve

Test Result Variable(s): SMAX

Area	Std. Error[a]	Asymptotic Sig.[b]	Asymptotic 95% Confidence Interval	
			Lower Bound	Upper Bound
.612	.078	.134	.460	.764

The test result variable(s): SMAX has at least one tie between the positive actual state group and the negative actual state group. Statistics may be biased.

a. Under the nonparametric assumption

b. Null hypothesis: true area = 0.5

The AUC is fairly significant to state that the OCT superior peripapillary NFL measurement corresponds well with the presence of an inferior hemifield visual field defect.

Chart 4 : Area under the receiver operator characteristic curve for OCT inferior peripapillary NFL measurements in patients with superior hemifield visual defects

ROC Curve
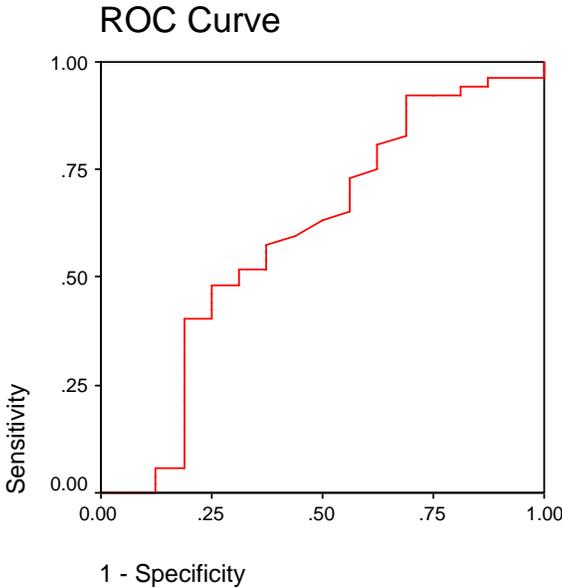
Area Under the Curve

Test Result Variable(s): IMAX

Area	Std. Error[a]	Asymptotic Sig.[b]	Asymptotic 95% Confidence Interval	
			Lower Bound	Upper Bound
.599	.089	.236	.423	.774

The test result variable(s): IMAX has at least one tie between the positive actual state group and the negative actual state group. Statistics may be biased.

a. Under the nonparametric assumption

b. Null hypothesis: true area = 0.5

The AUC is significant enough to state that OCT inferior peripapillary NFL measurements correspond well with superior hemifield visual field defects. But comparatively they are not as accurate as superior peripapillary NFL measurements in detecting disease.

DEMOGRAPHIC STUDY POPULATION CHARACTERISTICS

Table 1 : Age Distribution

Descriptive Statistics

	N	Minimum	Maximum	Mean	Std. Deviation
Age	38	10	67	45.00	11.409

Table 2 : Sex Distribution

Sex

	Frequency	Percent
Male	23	60.5
Female	15	39.5
Total	38	100.0

Table 3a : Distribution of Visual field defects with Reliability indices

Descriptive Statistics

		Visual Defect		
		No VF Defect	Single hemifield VF Defect	Both hemifield VF Defect
MEAND	eyes	18	41	11
	Mean	-1.4144	-5.1746	-13.6045
	Std. Deviation	3.67160	4.34579	9.65294
PATTD	eyes	18	40	11
	Mean	3.1433	5.9670	8.3736
	Std. Deviation	2.45162	2.95132	4.38503

Table 3 b :

ANOVA

		Sig.
MEAND	p-value	.000
PATTD	p-value	.000

MEAND= Mean Deviation, PATTD= Pattern Deviation, VF= Visual Field, ANOVA= Analysis of Variance.

Seventy-six eyes of 38 patients diagnosed with primary open angle glaucoma were included in the study. The mean age of the patients was 45 ±11.409 (Table 1). The gender ratio was 60.5% males and 39.5% females (Table 2). Of the 76 eyes, 18 had no demonstrable visual field defect, 41 eyes had visual field defects confined to one hemifield (superior or inferior), and 11 eyes had field defects in both eyes (Table 3a). The ANOVA (analysis of variance) for the mean and pattern deviation in these three groups of eyes (no VF defect, Single hemifield VF defect, both hemifield VF defect) was significant (p value <0.000) (Table 3b). The average mean deviation for these eyes was -5.4736 ±6.352, and average pattern deviation was 5.5081± 3.458.

The receiver operator characteristic curves were plotted using SPSS^{TM} and STRATA software. For the entire study group the AUC for optical coherence tomography peripapillary nerve fibre layer measurements in patients diagnosed with visually confirmed optic nerve head changes was 0.76 (Chart 1), which was high and significant (p value < 0.000). The AUC for optical coherence tomography NFL measurements in patients with visual field defects was 0.686 (Chart 2), which was also significant (p value = 0.01). But compared to the AUC for OCT in patients with optic nerve head changes, this area was lesser. OCT measurements also correlated well with the type of visual field defects. Higher AUCs were found for areas that correspond to the location of the visual field defect. Measurements of superior peripapillary NFL thickness

was significant in predicting the presence of inferior visual field defects (AUC was 0.612) (Chart 3) and measurements of inferior peripapillary NFL thickness was significant in predicting the presence of superior visual field defects (AUC was 0.599) (Chart 4). But when compared to superior peripapillary NFL measurements, inferior NFL measurements appear to be less accurate in predicting visual field defects.

DISCUSSION AND CONCLUSION

This study was done to evaluate a relatively new diagnostic modality – the Optical coherence tomography in the diagnosis and management of Primary Open Angle Glaucoma (POAG). To achieve this we evaluated the association between functional findings as determined by perimetry, and structural findings as measured by OCT Peripapillary Nerve Fibre Layer (NFL) thickness. The assessment also included the correlation of OCT NFL measurements with ophthalmoscopically visible optic nerve head changes.

The current study shows significant agreement of peripapillary NFL thinning measured by OCT and detection of glaucomatous optic nerve head changes by dilated slit lamp biomicroscopic fundus evaluation ($p<0.000$). High Area under Curve (AUC) (0.761) was found in the Receiver Operator Characteristic (ROC) for the peripapillary NFL thickness measurements in patients with primary open angle glaucoma with visible optic nerve head changes. In a significant number of eyes, i.e., 20.52 % (n=27) NFL thinning could be demonstrated by OCT even when visible optic nerve head changes could not diagnose the presence of POAG. This suggests that OCT could predict the onset of optic nerve head changes much before they become visible and may be used in the diagnosis of early glaucoma.

Several authors have investigated the correlation of quantitative assessment of nerve fibre layer thickness with conventional measurements of optic nerve structure and function[79,80, 81]. Bowd C et al[80] investigated 87 eyes, to conclude that NFL thickness was significantly thinner in glaucomatous eyes than in normal eyes in each quadrant. The study also mentioned that among all quadrants inferior quadrant OCT measured NFL defects show the closest relationship to glaucoma status followed by superior quadrant NFL defects.

When OCT was compared with the current gold standard of glaucoma detection, which is standard automated perimetry, the AUC was 0.686 for NFL thickness in eyes with visual field defects, suggesting significant correlation between the two (p=0.01). Previous studies have corroborated the fact that the NFL as measured by OCT was significantly thinned in regions coinciding with areas of visual field loss[82, 84, 85]. In our study, we compared the peripapillary NFL thickness in the superior and inferior poles (i.e., Smax and Imax, respectively) as they are the most related to glaucomatous visual field defect areas. It maybe speculated that assessing meridians in all 12 clock hours and comparing them with corresponding visual field zones may give much more specific results of correlation. But several authors have concluded that the NFL areas most frequently outside normal results were the inferior followed by superior peripapillary areas[82]. Hence we confined to assessment to these two specific areas.

The current study also shows a higher AUC for the ROC of OCT in optic nerve head changes (0.761) than the AUC for the ROC of OCT in visual field defects (0.686), pointing to the fact that OCT NFL measurements are a better diagnostic test than the standard automated perimetry. This is also compounded by the fact that many cases (n=27) with normal automated perimetry showed significant peripapillary NFL thinning by OCT. This would suggest that NFL thinning measured by OCT should be considered in early glaucoma and glaucoma suspect patients who may otherwise show normal visual fields by standard automated perimetry.

Glaucoma patients could suffer a loss (approx. 40%) of retinal ganglion cell axons before an automated perimetry visual field defect is evident. Hence an advanced imaging modality like OCT is warranted in the early detection and appropriate treatment of eyes with POAG, before valuable ganglion cells and visual fields are lost permanently.

The current study also compared the association of visual hemifield defects with corresponding hemiretina to study the correlation of OCT NFL measurements and visual fields by automated perimetry (superior hemifield defect association with inferior hemiretina NFL thinning and vice versa). The ROC curve for inferior hemifield defects with superior hemiretina NFL thinning showed significant area under the curve (0.612) but the area under the curve for the superior hemifield defect with inferior hemiretina NFL thinning

was not (0.599). This is in contrast to previous studies which showed most sensitive NFL areas to be inferior and inferotemporal areas. This might be because of smaller number of superior hemifield visual field defect cases which artificially appears to decrease its diagnostic efficacy.

The use of the Receiver Operator Characteristic curve to prove the accuracy of the diagnostic test has been done in various recent studies, showing similar area under the curve values. Williams ZY et al[83] also used ROC curves to determine if OCT measurements of NFL thickness can be used to predict the presence of visual field defects associated with glaucoma. The Area under the curve for NFL in patients with visual field defects was 0.73 and was found to be significant. The current study produces similar results with an AUC of 0.76 and was significant ($p<0.000$).

The limitation of this study is the lack of age matched controls from the normal population. It uses the pre-existing normative database of the machine in the presenting population of the clinic. A similar study with inclusion of normal population as age matched controls would possibly make the results more objectively specific. Inclusion of glaucoma suspects, ocular hypertensives and early glaucoma patients in subsequent trials in glaucoma diagnosis would make the use of OCT much more rewarding and provide the glaucoma specialist with an invaluable weapon in their armamentarium.

In conclusion, the current study establishes the fact that OCT peripapillary NFL thickness measurements are indeed an accurate and sensitive diagnostic modality for detecting primary open angle glaucoma. It is effective in diagnosing patients who have very early optic nerve head changes and may suffer permanent disc changes with the progression of the disease. In comparison with automated perimetry by Humphrey's visual field analysis, OCT corresponds well with the visual field defects defected. It is in fact more effective in predicting localized areas of NFL thinning before they may become manifest as visual field changes. Hence the use of OCT in POAG even before the appearance of visual field changes should be considered for the patient's advantage.

Optical coherence tomography illustrates cross-sectionally the activity occurring in the NFL, a site of particular interest in glaucoma. In this study, it demonstrated thinning of the OCT peripapillary NFL in areas corresponding to visual field defects and optic nerve head changes, in agreement with several previous studies.

OCT in the field of glaucoma may have a significant impact on its diagnosis and clinical management. In this way, the disease can be investigated a step closer to "where the action is," at the level of the NFL, as opposed to determining if there are fewer axons among the hundreds of thousands making up the optic nerve in the 1.5 mm scleral canal. By direct investigation of the

NFL with OCT, earlier diagnosis of glaucoma and earlier detection of glaucomatous progression should be possible, before conventional signs such as visual field loss, cupping of the optic nerve head, and NFL defects are evident, thus allowing earlier treatment and reducing the damage done by glaucoma.

BIBLIOGRAPHY

1. Quigley HA: Number of people with glaucoma worldwide. Br J Ophthalmol 80:389, 1996

2. Thylefors B, Negrel AD: The global impact of glaucoma. Bull world Health Organ 72: 323, 1994

3. American Academy of Ophthalmology: Primary open-angle glaucoma: preferred practice pattern, San Francisco, 1996, The Academy.

4. Schuman SJ et al: Quantification of Nerve Fibre layer thickness in normal and glaucomatous eyes using Optical Coherence Tomography. Arch Ophthalmol 113:586-596, 1995

5. Quigley HA, Addicks EM, Green WR. Optic nerve damage in human glaucoma, III: quantitative correlation of nerve fibre loss and visual field defect in glaucoma, ischemic neuropathy, papilledema, and toxic neuropathy. Arch Opthalmol. 1982; 100:135-146

6. Lichter PR. Variability of expert observers in evaluating the optic disc. Trans Am Ophthalmol Soc. 1976; 74:532

7. Mikelberg FS, Airaksinen PJ, Douglas GR, Schulzer M, Wijsman K., The correlation between optic disk topography measured by the videoophthalmograph (Rodenstock analyzer) and clinical measurement. Am J Ophthalmol. 1985; 100:417

8. Shields MB et al, Reproducibility of topographic measurements with the optic nerve head analyzer. Am J Ophthalmol. 1987; 104:581

9. Caprioli J et al., Reproducibility of optic disc measurements with computerized analysis of stereoscopic video images. Arch Ophthalmol. 1986; 104:1035-1039

10. Shields MB. The future of computerized image analysis in the management of glaucoma. Am J Ophthalmol. 1989; 108:319

11. Balazsi GA, et al. Neuroretinal rim area in suspected glaucoma and early chronic open-angle glaucoma. Arch Ophthalmol. 1984; 102:1011-1014

12. Airaksinen PF, Drance SM, Schulzer M., Neuroretinal rim area in early glaucoma. Am J Ophthalmol. 1985; 99:1

13. Caprioli J, et al. Videographic measurements of optic nerve topography in glaucoma. Invest ophthalmol Vis sci. 1988; 29:1294

14. Caprioli J, et al. Measurements of peripapillary nerve fibre layer contour in glaucoma. Am J Ophthalmol. 1989; 108:404

15. Bille JF, Dreher AW, Zinser G., Scanning laser tomography of the living human eye. In Masters BR, ed. Noninvasive Diagnostic Techniques in Ophthalmology. New York, NY: Springer-Verlag NY Inc; 1990; 29:1294

16. Huang D, Swanson EA, Lin CP, et al. Optical coherence tomography. Science 1991; 254:1178-1181

17. Hee MR, Izatt JA, Swanson EA, et al, Optical coherence tomography of the human retina. Arch Ophthalmol. 1995; 113:325-332

18. Chauhan DS, Marshall J. The interpretation of Optical coherence tomography images of the retina. Invest Ophthalmol Vis Sci 1999; 40:2332-2342

19. Pieroth L, Schuman JS, Hertzmark E, et al. Evaluation of focal defects of the nerve fibre layer using Optical coherence tomography: a pilot study. Arch Ophthalmol. 1995; 113:586-596

20. Zangwill LM, Williams J, Berry CC, et al., A comparison of Optical coherence tomography and retinal nerve fibre layer photography for detection of nerve fibre layer damage in glaucoma. Ophthalmology 1999; 106:570-579

21. Hon ST, Greenfield DS, Mistlberger A, et al. Optical coherence tomography and scanning laser polarimetry in normal, ocular hypertensive, and glaucomatous eyes. Am J Ophthalmol 2000; 129:129-135

22. Bowd C, Weinreb RN, Williams JM et al., The retinal nerve fibre layer thickness in ocular hypertensive, normal and glaucomatous eyes with Optical coherence tomography. Arch Ophthalmol 2000; 118:22-26

23. Soliman MAE, Van Den Berg TJTP, Ismaeil LA, et al. Retinal nerve fibre layer analysis: relationship between Optical coherence tomography and red-free photography. Am J Ophthalmol 2002; 133:187-195

24. Quigley HA, Dunkelberger GR, Green WR. Retinal ganglion cell atrophy correlated with automated perimetry in human eyes with glaucoma. Am J Ophthalmol 1989; 107; 453-464

25. Helmholtz H. Beschreiburg eines augenspiegels zur untersuchung der netzhaut in lebnden augie. Berlin, A. Forstner, 1851

26. Lichter PR. Variability of expert observers in evaluating the optic disc. Trans Am Ophthalmol Soc 1976;74:532

27. Tielsch JM, Schwartz B. Reproducibility of photogrammetric optic disc cup measurements. Invest Ophthalmol Vis Sci 1985;26:814

28. Varma R, Spaeth GL. The PAR IS 2000. A new system for retinal digital analysis. Ophthalmic Surgery 1988;19:1183

29. Dandona L, Quigley HA, Jampel HD. Reliability of optic nerve head topographic measurements with computerized image analysis. Am J Ophthalmol 1989;108:414

30. Bishop KI, Werner EB, Krupin T, et al. Variability and reproducibility of optic disc topographic measurements with the Rodenstock Optic Nerve Head Analyzer. Am J Ophthalml 1988;106:696

31. Belyea DA, Dan JA, Lieberman MF, et al. The Glaucoma-scope: Reproducibility and accuracy of results. Invest Ophthalmol Vis Sci 1994;35:429

32. Hamzavis S, Stewart WC, Thompson TL. Inter and intraobserver variation of the optic nerve head in cadaver eyes using the Glaucoma-scope. Invest Ophthalmol Vis Sci 1993;35 (suppl): 427

33. Takamoto T, Netland PA, Schwartz B. Comparison of measurements of optic disc cup by glaucoma scope and stereophotogrammetry. Invest Ophthalmol Vis Sci 1993;35(suppl): 433

34. Balazsi GA, Drance SM, Schulzer M, et al. Neuroretinal rim area in suspected glaucoma and early chronic open angle glaucoma. Arch Ophthalmol 1984;102:1011

35. Caprioli J, Ortiz-Colberg R, Miller JM, Tressler C. Measurements of Peripapillary nerve fibre layer contour in glaucoma. Am J Ophthalmol 1989;108:404

36. Shields MB, Martone JF, Shelton AR, et al. Reproducibility of topographic measurements with the optic nerve head analyzer. Am J Ophthalmol 1987;104:581

37. Shields MB, Tiedeman JS, Miller KN, et al. Accuracy of topographic measurements with the optic nerve head analyzer. Am J Ophthalmol 1989;107:273

38. Plesch A, Klingbeil U, Rappl W, et al. Scanning ophthalmic imaging. In Nasmann JE, Burk ROW (eds). Scanning laser ophthalmoscopy and tomography. Munchen, Quintessenz, 1990, p 23-37

39. Webb RH, Hughes GW, Delori FC. Confocal scanning laser ophthalmoscope. Applied Optics, 1987;26:1492

40. Peli E. Electro-optic fundus imaging. Surv Ophthalmol, 1989;34:113

41. Kino GS, Corle TR. Confocal scanning optical microscopy. Physics Today 1989;42:55

42. Masters BR, Kino GS. Confocal microscopy of the eye. In Masters BR (ed). Noninvasive Diagnostic Techniques in Ophthalmology. New York, Springer-Verlag, 1990, pp 152-171

43. Schuman H, Murray JM, Di Lullo C. Confocal microscopy. An overview. Bio Techniques 1989;7:154

44. Billie JF, Dreher GW, Zinser G. Scanning laser tomography of the living human eye. In Masters BR (ed); Noninvasive Diagnostic Techniques in Ophthalmology. New York, Springer-Verlag, 1990, pp 528-547

45. Dreher AW, Tso PC, Weinreib RN. Reproducibility of topographic measurements of the normal and glaucomatous optic nerve head with the laser tomographic scanner. Am J Ophthalmol, 1991;111:221

46. Mikelberg F, Wijsman K, Schulzer M. Reproducibility of topographic parameters obtained with the Heidelberg retina tomography. J Glaucoma, 1993;2:101-103

47. Quigley HA, Addicks EM, Green WR. Optic nerve damage in human glaucoma. Arch Ophthalmol 1982;100:135

48. Quigley HA, Addicks EM. Quantitative studies of retinal nerve fibre layer defects. Arch Ophthalmol 100:807-814,1982

49. Quigley HA, Miller NR, George T. Clinical evaluation of nerve fibre layer atrophy as an indicator of glaucomatous optic nerve damage. Arch Ophthalmol,1980;98:1564-1571

50. Reiter K, Dreher AW, Weinreb RN. Accuracy and reproducibility of a retinal laser ellipsometer. Invest Ophthalmol Vis Sci 1991;32(suppl):812

51. Dreher AW, Reiter K, Weinreb RN. Spatially resolved birefringence of the retinal nerve fibre layer assessed with a retinal laser ellipsometer. Applied Optics 1992;31:3730-3735

52. Weinreb RN, Dreher AW, Coleman A, et al. Histopathologic validation of Fourier-ellipsometry measurements of retinal nerve fibre layer thickness. Arch Ophthalmol 1990;108:557

53. Dreher AW, Reiter K. Retinal laser ellipsometry: A new method for measuring the retinal nerve fibre layer thickness distribution? Clinical Vision Sciences,1992;7: 481-488

54. Morsman CD, Karwatowski WSS, Wienreb RN. Reproducibility of retinal nerve fibre layer thickness measurements by scanning laser polarimetry and correlation with red free photography in normal eye. Invest Ophthalmol Vis Sci 1993;34(suppl):1507

55. Zeimer R, Shahidi M, Mori M, et al. A new method for rapid mapping of the retinal thickness at the posterior pole. Invest Ophthalmol Vis Sci 1996;37:1994-2001

56. Schuman JS, Kim Joshua, Imaging of the optic nerve head and nerve fibre layer in glaucoma. Ophthalmol Clinics of North America, 2000;13:383-406

57. Schuman JS, Noecker RJ, Imaging of the optic nerve head and nerve fibre layer in glaucoma. Ophthalmol clinics of North America, 1995; 8:259-280

58. Olsen T. The accuracy of ultrasonic determination of axial length in pseudophakic eyes. Acta Ophthalmol (Copenh) 1989; 67:141-144

59. Pavlin DJ, Sherar MD, Foster FS. Subsurface ultrasound microscopic imaging of the intact eye. Ophthalmology 1990; 7:244-250

60. Pavlin CJ, et al. Clinical use of ultrasound biomicroscopy. Ophthalmology. 1990; 98:287-295

61. Chang DF. Ophthalmic examination. In: General Ophthalmology. 13th ed. 1992:30-62

62. Seiler T, Bende T. Magnetic resonance imaging of the eye and orbit. Noninvasive Diagnostic Techniques in Ophthalmology. 1990:17-31

63. Webb RH, et al. Confocal scanning laser ophthalmoscope. Appl Opt. 1987;26:1492-1499

64. Bille JF et al. Scanning laser tomography of the living human eye. Noninvasive

    Diagnostic Techniques in Ophthalmology. 1990:528-547

65. Hee MR et al. Optical Coherence Tomography of the Human Retina. Arch Ophthalmol. 1995; 113:325-332

66. Werner EB, Interpreting automated visual fields. Ophthalmology Clinics of North America. 1995; 8:229-258

67. Heijl A et al. Extended empirical statistical package for evaluation of single and multiple fields in glaucoma: Statpac2. Perimetry update 1991, pp 303-315

68. Heijl A: Reliability parameters in computerized perimetry. Seventh International Visual Field Symposium, 1987, pp 593-600

69. Heijl A: A package for the statistical analysis of visual fields. Seventh International Visual Field Symposium, 1987, pp 153-168

70. Flammer J. The concept of visual field indices. Graefes Arch Clin Exp Ophthalmol, 1986; 224:389-392

71. Heijl A, et al. A package for the statistical analysis of visual fields. Seventh International Visual Field Symposium, 1987, pp 153-168

72. Aman P, Heijl A. Glaucoma hemifield automated visual field evaluation. Arch Ophthalmol 1992; 110: 812-819

73. Asman P, Heijl A. Evaluation of methods for automated hemifield analysis in perimetry. Arch Ophthalmol 1992; 110: 820-826

74. Anderson DR. Automated Static Perimetry. St. Louis, MO, Mosby Year Book 1992, pp 10-93

75. Radius RL. Anatomy and pathophysiology of the retina and the optic nerve. The Glaucomas. St. Louis, CV Mosby, 1989, pp 89-132.

76. Lindenmuth KA, et al. Effects of papillary constriction on automated perimetry in normal eyes. Ophthalmology, 1989; 96:1298-1301

77. Searle AET, Wild JM, Shaw DE, et al. Time-related variation in normal automated perimetry. Ophthalmology 1991; 98: 701-707

78. Obuchowski Nancy A., Receiver Operating Characteristic curves and their use in Radiology, 2003; 229: 3-8

79. Schuman JS, et al. Quantification of Nerve Fibre Layer Thickness in Normal and Glaucomatous Eyes Using Optical Coherence Tomography. Arch Ophthalmol. 1995; 113: 586-596

80. Bowd C et al. The Retinal Nerve Fibre Layer Thickness in Ocular Hypertensive, Normal and Glaucomatous Eyes with Optical Coherence Tomography. Arch Ophthalmol. 2000; 118 : 22-26

81. Kanamori A, Nakamura M, Escano MF, et al. Evaluation of the glaucomatous damage on retinal nerve fibre layer thickness measured by optical coherence tomography. Am J Ophthalmol. 2003;135:513-520

82. El Beltagi TA, Bowd C, Boden C,et al. Retinal Nerve Fibre Layer Thickness Measured with Optical Coherence Tomography is Related to Visual Function in Glaucomatous Eyes. Ophthalmology 2003;110:2185-2191

83. Williams ZY, Schuman JS, Gamell L et al. Optical Coherence Tomography Measurement of Nerve Fibre Layer Thickness and the Likelihood of a Visual Field Defect. Am J Ophthalmol 2002; 134:538-546

84. Mok KH, Lee VW, So KF et al. Retinal Nerve Fibre Layer Measurement by Optical Coherence Tomography in glaucoma suspects with short-wavelenght perimetry abnormalities. J Glaucoma. 2003;12:45-49

85. Sanchez-Galeana CA, Bowd C, Zangwill LM, et al. Short Wavelength automated perimetry results are correlated with optical coherence tomography retinal nerve fibre layer thickness measurements in glaucomatous eyes. Ophthalmology, 2004;111:1866-1872

Figure 2 : The CARL ZEIS STRAUSS Optical Coherence Tomography

Optical Coherence Tomography

Figure 3 : Patient Examination on Optical Coherence Tomography

Figure 4 : Optic Nerve Head Evaluation by OCT

Figure 5 : Optic Nerve Head Cross Section

Fig 6 : RNFL THICKNESS AVERAGE ANALYSIS

Sectoral Analysis

Tabulated Analysis

OD

OS

Microns — TEMP SUP NAS INF TEMP

— OD   -----OS

	OD (N=3)	OS (N=3)	OD-OS
Imax/Smax	0.98	0.97	0.01
Smax/Imax	1.02	1.03	-0.01
Smax/Tavg	1.83	2.34	-0.51
Imax/Tavg	1.79	2.27	-0.48
Smax/Navg	2.08	2.88	-0.80
Max-Min	69.00	94.00	-25.00
Smax	110.00	126.00	-16.00
Imax	107.00	122.00	-15.00
Savg	67.00	78.00	-11.00
Iavg	80.00	84.00	-4.00
Avg.Thickness	64.81	64.75	0.06

Normal distribution Percentiles
100%
95%
5%
1%
0%

Patient/Scan Information

Karuppasamy
A

DOB: 7/1/1945, ID: 2036726, Male

Scan Type	Fast RNFL Thickness (3.4)
Scan Date	3/16/2005
Scan Length	10.87 mm

Signal Strength (Max 10)   9

Signal Strength (Max 10)   10

ZEISS

Fig 7: Correlation of ONH changes and Visual Fields with Optical Coherence Tomography

Optical Coherence Tomography

Visual Field

Fundus Photograph

Normal Eye

Glaucomatous Eye

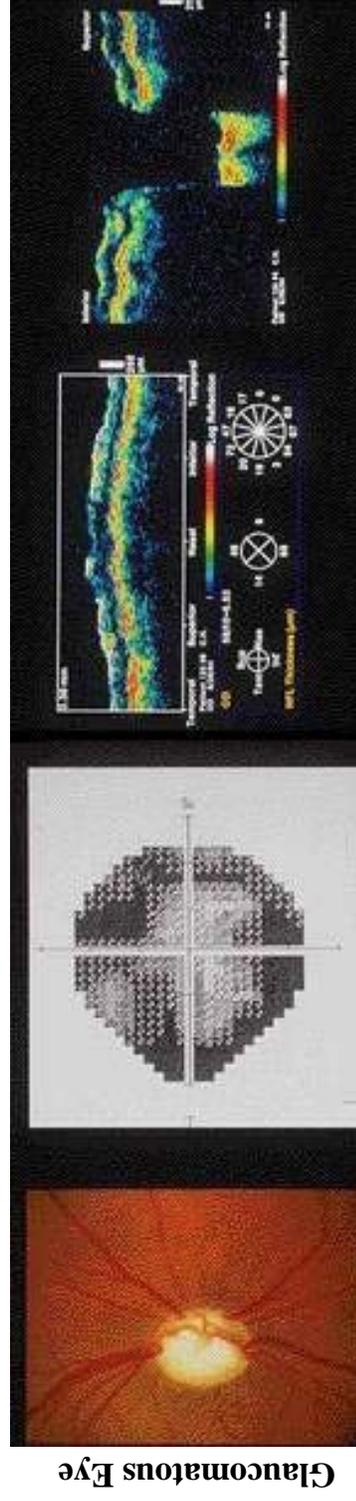| Sno	Name	Age	Sex	Medical Record No.	UCVA RE	UCVA LE	BCVA RE	BCVA LE	IOP RE	IOP LE	CUP/DISC RE	CUP/DISC LE	Notching RE	Notching LE	Disc hge RE	Disc hge LE	NFL Defect RE	NFL Defect LE	Field defect RE	Field defect LE	Mean Deviation RE	Mean Deviation LE	Pattern Deviation RE	Pattern Deviation LE	OCT Smax RE	OCT Smax LE	OCT Imax RE	OCT Imax LE	Avg. thickness RE	Avg. thickness LE
1	KASTHURI.N	55	2	1942545	6/36	6/36	6/6	6/6	16	16	0.60	0.70	2	3	1	2	1	2	2	3	-6.77	-9.46	8.60	12.06	160.0	149.0	179.0	123.0	93.58	81.06
2	RENGASAMY	38	1	2020775	6/6	6/6			30	30	0.90	0.85	1	1	1	1	3	2	2	2	-11.93	-11.66	8.34	8.50	119.0	125.0	97.0	111.0	72.00	79.04
3	JAMES.M	45	1	1966383	6/6	6/6			14	16	0.80	0.80	1	2	1	1	1	3	1	1	3.28	-0.12	3.53	3.64	148.0	140.0	126.0	134.0	88.91	75.62
4	DEVADASS	50	1	1006239	6/6P	6/6	6/6P	6/6	20	20	0.65	0.85	1	1	1	1	1	2	1	4	0.44	-3.14	1.53	6.07	162.0	118.0	166.0	89.0	117.00	77.00
5	SHEBA SHUTOOR	32	2	1967263	6/9	6/60	6/6	6/6	10	9	0.70	0.60	2	2	1	1	1	1	3	1	-2.59	-1.23	6.63	1.98	106.0	123.0	193.0	176.0	89.95	91.47
6	SHOBA NAIR	39	2	1151484	6/12	6/9	6/6	6/6	12	10	0.75	0.50	3	1	1	1	1	1	2	1	-2.34	0.68	7.30	1.42	127.0	169.0	114.0	164.0	81.38	95.70
7	SAKUNDALA SELVARAJ.S	56	2	1609107	6/9	6/9	6/6	6/6	16	18	0.80	0.60	2	3	1	1	1	1	5	5	-11.13	-13.22	8.33	10.66	110.0	165.0	112.0	182.0	74.80	101.88
8	GURUSAMY.N	32	1	941288	6/6	6/6			16	12	0.75	0.50	2	1	1	1	1	1	3	3	-8.10	-7.10	8.77	7.32	83.0	175.0	156.0	153.0	79.80	101.69
9	MANI.K	53	1	1940776	6/12	6/12	6/6	6/6	13	14	0.75	0.80	3	3	1	1	2	1	2	2	-8.21	-6.36	11.80	8.90	105.0	51.0	64.0	64.0	54.72	44.04
10	AMUTHAVENI.P	35	2	1514437	5/60	5/60	6/6	6/6	20	19	0.75	0.75	3	1	1	1	1	1	4	2	-1.51	-2.32	2.36	2.72	134.0	163.0	115.0	139.0	84.71	95.78
11	KALPANA	58	2	1671211	6/60	6/36	6/9	6/6	20	18	0.70	0.40	3	1	1	1	1	1	1	1	-5.37	-3.88	2.47	1.77	123.0	104.0	171.0	151.0	85.54	80.44
12	HERIC MANI	49	1	2000737	6/6	6/6			20	20	0.80	0.80	3	3	1	1	1	1	2	1	-2.65	-1.16	4.06	1.73	107.0	124.0	148.0	149.0	74.28	81.50
13	BABU.G	38	1	1773110	2/60	2/60	6/12	6/9	25	20	0.80	0.85	1	1	1	1	1	1	4	3	-13.42	-23.57	9.90	11.98	59.0	58.0	53.0	52.0	38.91	41.58
14	MOIDEEN KOYA.CP	39	1	1935527	6/6	6/6			16	16	0.70	0.80	1	1	1	1	1	1	3	3	-8.58	-5.33	9.71	3.43	166.0	79.0	120.0	109.0	86.99	63.53
15	VARSHINI	10	2	1659821	6/6	6/6			14	13	0.80	0.50	1	1	1	1	4	1	1	1	-3.60	1.00	7.28		111.0	157.0	125.0	121.0	59.32	98.25
16	RAJENDRAN.R	50	1	1841422	6/9	6/6	6/6		28	28	0.60	0.60	1	1	1	1	2	1	1	1	0.56	0.68	1.22	1.37	191.0	176.0	162.0	168.0	93.77	94.70
17	UMAKASI RANI	50	2	1499777	6/60	6/36	6/6	6/6	18	18	0.65	0.75	1	3	1	1	1	1	5	1	-16.61	-2.16	15.38	4.04	135.0	125.0	112.0	100.0	82.70	77.10
18	JOHSPHINE MARY	67	2	1970944	6/36	6/36	6/6	6/6	14	16	0.80	0.85	1	1	1	1	1	1	3	3	-4.68	-6.25	3.08	5.58	96.0	77.0	99.0	102.0	73.98	57.09
19	MOHAMED KUNDHI	56	1	1970890	6/60	6/60	6/6	6/6	12	14	0.80	0.75	1	1	1	1	3	1	3	1	-11.58	-8.34	6.06	5.54	143.0	145.0	120.0	133.0	76.98	81.58

Sno	Name	Age	Sex	Medical Record No.	UCVA		BCVA		IOP		CUP/DISC		Notching		Disc hge		NFL Defect		Field defect		Mean Deviation		Pattern Deviation		OCT Smax		OCT Imax		Avg. thickness	
					RE	LE	RE	LE	RE	LE	RE	LE	RE	LE	RE	LE	RE	LE	RE	LE	RE	LE	RE	LE	RE	LE	RE	LE	RE	LE
20	VISALAM.P	60	2	1650557	6/60	6/60	6/6	6/9	14	18	0.50	0.70	1	3	1	1	1	1	1	2	1.69	-2.93	1.51	6.80	135.0	141.0	189.0	136.0	93.11	78.88
21	SOMASUNDARAM	50	1	1748319	6/60	6/60	6/9	6/9	18	16	0.70	0.90	1	1	1	1	1	5	1	5	0.35	-21.85	1.01	13.94	162.0	93.0	114.0	66.0	81.37	49.32
22	SREENIVASAN REDDY	25	1	1843878	5/60	5/60	6/6	6/6	28	22	0.70	0.60	1	1	1	1	1	1	2	1	-9.00	-1.83	4.30	2.98		90.0		110.0		77.70
23	RAMESWARI	34	2	1534266	6/36	6/36	6/6	6/6	24	16	0.30	0.30	1	1	1	1	1	1	3	1	-8.17	-0.79	11.57	3.32	139.0	126.0	142.0	140.0	87.62	73.89
24	HARIKAUTH	38	1	1840149	6/12	6/12	6/6	6/6	20	18	0.75	0.65	1	1	1	1	1	1	1	1	-1.64	0.47	3.90	5.09	160.0	173.0	171.0	160.0	106.60	99.01
25	SOUNDARARAJA PERUMAL	44	1	1842101	6/6	6/6			28	26	0.50	0.55	1	1	1	1	2	1	1	1	-9.49	-5.21	6.68	4.53	128.0	142.0	115.0	163.0	76.54	95.79
26	RATHINAVEL	50	1	1510029	6/12	6/9	6/6	6/6	20	20	0.50	0.75	1	1	1	1	3	6	2	3	-5.80	-18.66	5.13	9.99	128.0	84.0	130.0	101.0	85.83	54.13
27	MEGACHANDRA SINGH	42	1	1926714	4/60	4/60	6/6	6/6	14	12	0.75	0.60	3	1	1	1	2	1	2	1	-6.09	-2.28	9.78	4.84	121.0	142.0	95.0	125.0	59.93	77.37
28	MICHAEL RAVI	42	1	1919605	6/9	6/6	6/6	6/6	24	22	0.60	0.70	1	3	1	1	1	1	1	1	-0.50	-0.32	1.98	3.48	84.0	120.0	143.0	111.0	67.10	68.64
29	MAHENDRA SINGH RAJ	31	1	1668521	6/12	6/9	6/6	6/6	16	18	0.30	0.50	1	1	1	1	1	1	1	3	-2.31	-6.65	3.51	6.18	150.0	171.0	161.0	173.0	106.52	103.50
30	KAUSALYA GAURANG	55	2	2059113	6/6	6/6			22	20	0.50	0.70	1	1	1	1	1	1	5	5	-18.85	-30.77	10.95	6.37	121.0	70.0	131.0	113.0	66.80	59.31
31	POTHIRAJ	41	1	2027650	6/12	6/12	6/6	6/6	18	18	0.75	0.60	1	1	1	1	1	1	7	7	-4.42	-4.35	1.82	1.58	170.0	175.0	192.0	176.0	93.22	49.50
32	ARUMUGAM	42	1	1304728	6/6	6/6			16	16	0.75	0.85	1	1	1	1	1	1	3	3					125.0	128.0	161.0	147.0	94.30	87.07
33	ABIA RUTH ANNATHAI	65	2	1882436	6/12	6/9	6/6	6/6	18	18	0.75	0.70	1	1	1	1	1	1	2	2	-4.78	-3.28	5.16	5.52	98.0	125.0	82.0	125.0	59.11	79.82
34	KARUPPAIAH	55	1	417709	6/6	6/6			14	16	0.70	0.75	1	1	1	1	1	1	2	1	-5.01	4.75	3.97	2.53	138.0	148.0	126.0	126.0	88.00	81.00
35	VARGHESS.T.S	52	1	1849883	6/9	6/9	6/6	6/6	16	16	0.70	0.60	1	1	1	1	1	1	2	2	-4.75	-3.73	4.98	4.06	155.0	172.0	207.0	196.0	96.87	114.42
36	RADHAKRISHNAN	40	1	2021705	6/6	6/6			12	14	0.70	0.80	1	1	1	1	1	1	3	3	-3.80	-4.90	5.82	5.47	145.0	114.0	172.0	157.0	95.46	89.21
37	AYSATH KANNILA	40	2	2014271	6/6	6/6			18	18	0.65	0.70	3	1	2	1	1	1	1	1	0.20	-0.88	1.49	4.23	150.0	144.0	130.0	138.0	89.36	88.06
38	SAVITHIRI.K	52	2		6/6	6/6			14	14	0.70	0.70	1	1	1	1	1	1	1	1	-0.97	-0.77	1.48	1.08	119.0	149.0	138.0	165.0	75.49	75.92